

ISSN 1840-4855  
e-ISSN 2233-0046

Original scientific article  
<http://dx.doi.org/10.70102/afts.2024.1631.049>

## INFLUENCE AND PREDICTION OF SINTERED AGGREGATE SIZE DISTRIBUTION ON THE PERFORMANCE OF LIGHTWEIGHT ALKALI-ACTIVATED CONCRETE

Pushpendra Singh Palash<sup>1\*</sup>, Priyanka Dhurvey<sup>2</sup>

<sup>1\*</sup>Research Scholar, Department of Civil Engineering, MANIT-Bhopal, Madhya Pradesh.  
e-mail: palash.rgpv@gmail.com, orcid: <https://orcid.org/0000-0002-9074-1683>

<sup>2</sup>Assistant Professor, Department of Civil Engineering, MANIT-Bhopal, Madhya Pradesh.  
e-mail: pdhurvey@gmail.com, orcid: <https://orcid.org/0000-0003-4840-7144>

### SUMMARY

The most effective method for mitigating the adverse environmental impacts of traditional concrete involves substituting cement and natural aggregate with waste and byproduct resources. Utilizing sintered lightweight aggregate (fly ash) in geopolymer concrete emerges as an efficient solution for managing and disposing of significant amounts of fly ash. The influence of sintered aggregate size distribution on the performance of alkali-activated concrete, focusing on compressive strength improvement. The study employs sintered fly ash aggregate (SFA) as coarse aggregate, aiming to optimize packing density through proper particle distribution. The highest compressive strength is achieved with a mix featuring 75% 4-8mm and 25% 8-12mm SFA. Regression-based strength models are developed, exhibiting good alignment with conventional concrete models. Thin section techniques reveal enhanced aggregate-matrix interaction due to the porous structure of SFA. The study emphasizes the potential of SFA in geopolymer concrete for sustainable construction. Lightweight geopolymer concrete, owing to its lower density, significantly reduces the overall structural load.

**Key words:** *surveillance sintered fly ash aggregate, sustainable resource, compressive strength, regression analysis, geopolymer concrete, thin section techniques.*

*Received: June 10, 2024; Revised: August 09, 2024; Accepted: September 02, 2024; Published: October 30, 2024*

### INTRODUCTION

Concrete, the world's most widely used building material, increasingly incorporates lightweight concrete (LWC) for its versatile applications in intelligent infrastructure development [3]. Unlike conventional concrete with a mass density of 2200–2400 kg/m<sup>3</sup>, LWC ranges from 300–1900 kg/m<sup>3</sup> [1, 2], reducing dead load, enhancing thermal and acoustic insulation, and minimizing haulage costs. LWC finds diverse uses in engineering, including construction, bridge deck pavements, and architectural elements, categorized as structural lightweight, non-load-bearing, or insulating concrete, each offering higher specific strength.

Researchers have extensively studied the environmental impact of natural aggregate excavation, prompting the exploration of fly ash waste recycling as an aggregate to save landfill space and conserve natural resources.

This practice contributes to decreasing the construction industry's carbon footprint. The potential use of sintered fly ash aggregate (SFA) in concrete, controlled by various researchers, is established. This study specifically evaluates the performance of fly ash aggregate as coarse aggregates in Alkali-Activated Concrete, focusing on factors like packing density and aggregate distribution for superior load-carrying capacity compared to natural aggregates an aspect not reported previously, to the best of the author's knowledge.

## SCOPE OF INVESTIGATIONS AND EXPERIMENTAL PROGRAM

A comprehensive understanding of how sintered aggregate size distribution affects the properties of alkali-activated concrete is vital for optimizing mix designs and enhancing the applicability of this sustainable construction material in various engineering applications.

The findings of this study will contribute to the ongoing efforts to develop environmentally friendly and high-performance alternatives to conventional concrete, advancing the field of alkali-activated materials and promoting sustainable practices in the construction industry. The study involved selecting samples based on packing density with varying percentage combinations for coarse aggregates. Through statistical regression, prediction models were formulated to assess the mechanical strength of geopolymer concrete across different samples, accounting for particle size grading concerning age. The main procedures in producing geopolymer concrete, offering a concise overview of the experimental program conducted in this research.

## MATERIALS

### Aggregates

Fly ash, a byproduct of coal combustion in power plants, finds valuable application in construction materials like concrete and aggregates, contributing to the beneficial reuse of this industrial waste and fostering sustainable practices. Renowned for enhancing concrete strength and durability, fly ash aggregates engage in a pozzolanic reaction with calcium hydroxide during cement hydration, resulting in a denser and more resilient concrete matrix. The incorporation of fly ash in construction materials reduces the reliance on traditional cement production, a notable source of carbon dioxide emissions. Substituting a portion of cement with fly ash aids in lowering the overall carbon footprint of the construction industry. Additionally, fly ash aggregates improve the workability of concrete, streamlining placement and finishing processes, leading to enhanced construction efficiency and reduced labor requirements. Furthermore, concrete containing fly ash aggregates often displays improved thermal properties, contributing to energy efficiency in buildings by offering better insulation and reducing the need for additional heating or cooling. Many regions advocate or mandate the use of fly ash in construction materials due to its environmental advantages, aiding construction projects in compliance with regulations related to waste reduction and sustainability. Coarse aggregates in this study consist of Sintered Fly ash Lightweight Aggregates (SFA), manufactured by IS CODE 9142 PART 2. These artificially created aggregates possess a round shape, a hard interior, and honeycombed spongy structures resulting from thermal processing. Notably, these hard aggregates offer increased consistency and superior quality, while being up to 50% lighter than natural aggregates. Table 1 outlines SFA's physical characteristics, Figure 3 presents the XRD analysis, and Figure 4 the microstructure. Figure 1 shows the SFA used in this study was procured from Litagg Industries Private Limited, Ahmedabad, INDIA. As for fine aggregates, natural sand with a maximum particle size of 4.75 mm was employed. Physical characteristics of the fine aggregate are provided in Table 1 & 2.



Size (4-8mm)

Size (8-12mm)

Figure 1. Sintered fly ash aggregate (SFA)

Table 1. Physical characteristics of SFA

Properties	Value
Aggregate size	4-8mm; 8-12mm
Aggregate strength	More than 40MPa
Bulk density	@ 850Kg/M <sup>3</sup>
Bulk porosity	35-40%
Water absorption	17%
Aggregate shape	Rounded pallets

Table 2. Physical properties of natural sand

Properties	Value
Color	Brown
Water Absorption	0.98%
Specific Gravity	2.69
Particle Shape	Irregular
Grading of sand	Zone II
Silt Content	4.30%
Fineness modulus	2.39

### Fly Ash

Fly ash is a heterogeneous by-product, and to produce geopolymers, low-calcium fly ash (Class F) from coal-fired power stations is an appropriate resource. The practically spherical shape of fly ash particles allows for free flow and effective combination with other ingredients in mixes, making it a suitable binder for concrete. Due to its low calcium content, heat curing is required to accelerate the polymerization process, typically at temperatures ranging from 45 to 90°C [10]. The low calcium content also results in a longer initial setting time, necessitating heat curing to achieve early strength. The chemical characteristics of the fly ash used as a binder are provided in Table 3.

Table 3. Chemical composition of fly ash and GGBS

Properties	Chemical Composition (%)	Fly ash	GGBS
	SiO <sub>2</sub>	55	35.8
	Al <sub>2</sub> O <sub>3</sub>	26	13.46
	Fe <sub>2</sub> O	7	0.31
	CaO(Lime)	9	41.7
	MgO	2	5.99
	SO <sub>3</sub>	1	2.74

Due to its consistent fineness, distinctive particle shape, and reduced relative density, Ground Granulated Blast Furnace Slag (GGBS) demonstrates excellent mobility properties. Its glassy and smooth surface not only enhances texture and workability but also prevents efflorescence and staining in concrete. GGBS-based Geopolymer concrete achieves substantial initial strength at ambient temperature, attributed to its significant calcium content. This eliminates the necessity for heat curing to attain early strength, and in the present study, curing is conducted at ambient temperature. Additionally, when exposed to ambient curing conditions, Ground Granulated Blast Furnace Slag (GGBFS) accelerates the setting time of geopolymer concrete [4]. Table 3 provides an overview of the chemical characteristics of GGBS.

### Experimental Program

The components of geopolymer concrete comprise fly ash and Ground Granulated Blast Furnace Slag (GGBS) as binders, natural sand as fine aggregate, Sintered Fly ash (SFA) as coarse aggregate and an alkaline solution. The alkaline solution is crafted by blending sodium hydroxide pellets with a sodium silicate solution [17]. Conforming to the mix design specified in IS 10262:2019 for M-50 conventional cement concrete, a geopolymer concrete (GPC) is formulated with an identical mix ratio as conventional concrete, aiming for a characteristic compressive strength of 58.25 N/mm<sup>2</sup>[6]. Figure 2 provides a visual representation of slump values for various mixes. Throughout the study, the geopolymer mix

composition remains constant, featuring an alkaline liquid-to-binder ratio of 0.7%, sodium hydroxide to sodium silicate ratio of 2.0, a NaOH molarity of 12.5, a GGBS and fly ash blend in a 70:30 ratio, and initial and final setting times of 35 minutes and 50 minutes, respectively shows in table 4 & 5[4,12].

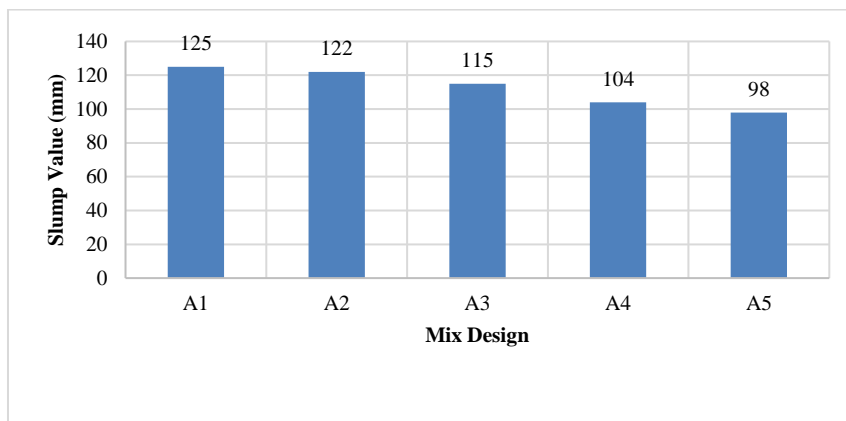


Figure 2. Slump values of different mixes

Table 4. Physical properties of a different mix of SFA

S. No.	Mix	Sample	% Combination	Specific Gravity	The volume of Voids %	Packing Density %	Water Absorption
1	Unitary	A <sub>1</sub>	(4-8mm=100%) & (8-12mm=0%)	1.771	55.67	0.443	19.46
2		A <sub>5</sub>	(4-8mm=0%) & (8-12mm=100%)	1.779	55.44	0.442	19.07
3	Binary	A <sub>2</sub>	(4-8mm=75%) & (8-12mm=25%)	1.796	56.03	0.446	19.50
4		A <sub>3</sub>	(4-8mm=50%) & (8-12mm=50%)	1.772	56.14	0.440	18.57
5		A <sub>4</sub>	(4-8mm=25%) & (8-12mm=75%)	1.775	55.82	0.439	21.59

Table 5. Configuration of coarse aggregate in concrete mixes [7]

Materials		Quantity in Kg				
		A <sub>1</sub>	A <sub>2</sub>	A <sub>3</sub>	A <sub>4</sub>	A <sub>5</sub>
GGBS and fly ash		567	567	567	567	567
Fine aggregate		889	889	889	889	889
Coarse aggregate	4-8mm	554	416	277	139	0
	8-12mm	0	139	277	416	554
Alkaline solution		340	340	340	340	340

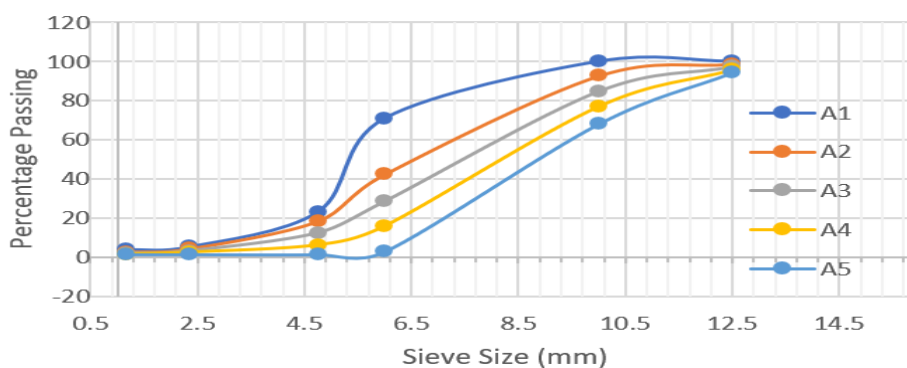


Figure 3. Gradation curve for different coarse aggregate configurations

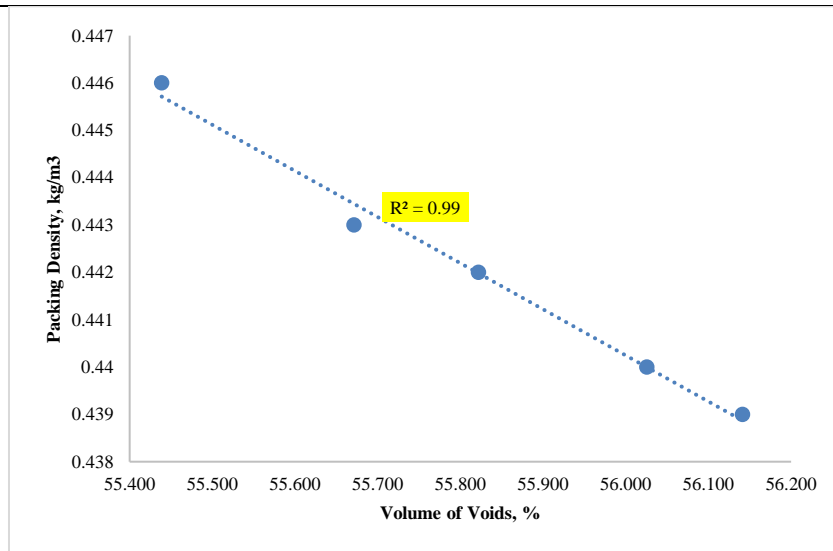


Figure 4. Relationship between the SFA packing density and void volume.

In Figure 4, the well-stretched straight trendline visually demonstrates the inverse correlation between the packing density of compacted SFA samples across various combinations and the percentage volume of voids.

## RESULTS & DISCUSSION

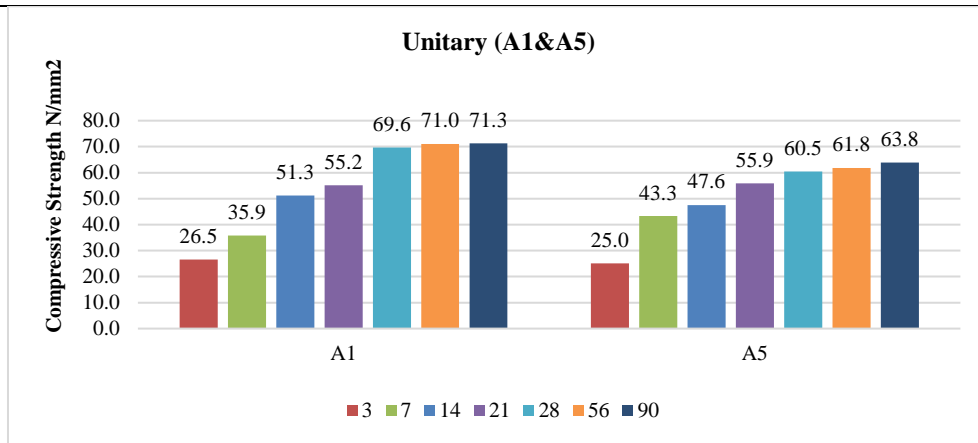
### Compressive Strength

Figures 4(a) and 4(b) present the compressive strength results for geopolymer concrete samples A<sub>1</sub>, A<sub>2</sub>, A<sub>3</sub>, A<sub>4</sub>, and A<sub>5</sub>. Notably, the A<sub>2</sub> mix, characterized by a combination of (4-8mm=75%) and (8-12mm=25%), exhibits maximum strength, owing to its well-graded aggregates. Across all mixes, there is a consistent trend of strength development over time, with each reaching the characteristic compressive strength values. A noteworthy observation from Table 6 is that many mixes achieve nearly 90% of the 28-day strength within a mere 21 days [16].

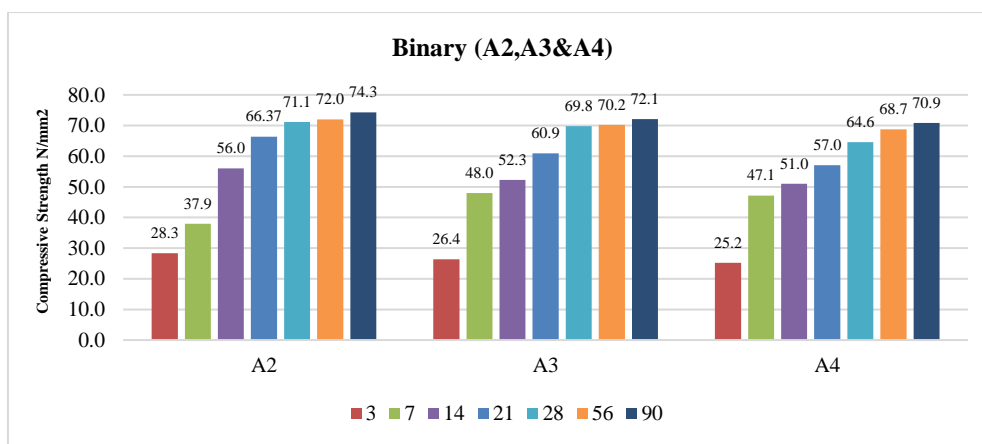
These variations in compressive strength are not solely attributable to aggregate strength; rather, they are intricately connected to physical and chemical processes occurring in the interfacial region. The early-stage absorption of gel by aggregates results in the densification of the interfacial transition zone—a physical process. Additionally, the accumulation of calcium hydroxide crystals in the outer shell of aggregates initiates a chemical reaction [14]. The accelerated strength development is attributed to an enhanced load transfer mechanism between the N-A-S-H gel (geopolymer gel) and the SFA. Studies on structural Lightweight Aggregate Concrete (LWAC) [Yu et al., 2013] and other types of lightweight aggregates (LWAs) [3] propose that faster strength development occurs as the N-A-S-H gel penetrates the surface pores of the SFA.

Table 6. Strength development of GP with SFA

Mix	Compressive Strength (MPa)							Strength Ratio (%)		
	3d	7d	14d	21d	28d	56d	90d	7d/28d	21d/28d	90d/28d (% gain)
A <sub>1</sub>	26.5	35.9	51.3	55.2	69.6	71	71.3	51.58	79.31	2.44
A <sub>2</sub>	28.3	37.9	56	66.37	71.1	72	74.3	53.31	93.35	4.50
A <sub>3</sub>	26.4	48	52.3	60.9	69.8	70.2	72.1	68.77	87.25	3.30
A <sub>4</sub>	25.2	47.1	51	57	64.6	68.7	70.9	72.91	88.24	9.75
A <sub>5</sub>	25	43.3	47.6	55.9	60.5	61.8	63.8	71.57	92.40	5.45
<b>Average</b>								63.63	88.11	5.09



(a) A1 & A5(Unitary)



(b) A2, A3 & A4 (Binary)

Figure 5. Compressive strength with different packing densities & percentage combination of SFA at different curing ages

In the current study, a regression-based model  $F_c(d)$  is developed to estimate the compressive strength of concrete with varying percentages of SFA at different curing ages in Figure 5. Using the 28th-day compressive strength,  $F_c(28)$ , and the normalized compressive strength generated by using the 28th-day strength, the model equation is derived. [8,9]. In geopolymer concrete (GP), factors such as fly ash type, alkaline solution, curing method, and temperature influence compressive strength. Standard ambient curing conditions are maintained throughout the experiments for the estimation of the strength evaluation model [5]. The equations for  $F_c(d)/F_c(28)$  are determined based on the experimental findings, utilizing the best-fitted regression analysis curve.

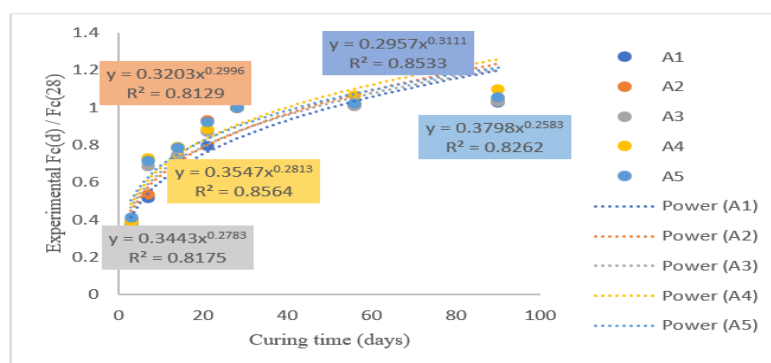


Figure 6. Compressive strength normalizes at 28days with curing age in days for A1, A2, A3, A4, & A5

A relationship between the ratio of experimental compressive strength data at any age, d (in days,  $F_c(d)$ ), to the 28th-day compressive strength  $F_c(28)$ , versus curing time (in days), is plotted in Figure 6 to derive the strength evaluation model for various samples. Regression was employed to construct five well-fitted power curves, resulting in the following generalized equation for compressive strength evaluation:

$$F_c(d)/F_c(28)=a_1t^{b_1} \tag{i}$$

where, t is the curing time,  $a_1$  and  $b_1$  are constants.

Because of higher  $R^2$  values, we can say constants  $a_1$  and  $b_1$  are proposing the compressive strength evaluation and they are rewritten as Eqs. for different samples A<sub>1</sub>, A<sub>2</sub>, A<sub>3</sub>, A<sub>4</sub>, and A<sub>5</sub>, respectively.

$$F_c(d)/F_c(28) = 0.265d^{0.395} \quad R^2 = 0.948 \tag{ii}$$

$$F_c(d)/F_c(28) = 0.226d^{0.446} \quad R^2 = 0.992 \tag{iii}$$

$$F_c(d)/F_c(28) = 0.263d^{0.403} \quad R^2 = 0.932 \tag{iv}$$

$$F_c(d)/F_c(28) = 0.264d^{0.400} \quad R^2 = 0.914 \tag{v}$$

$$F_c(d)/F_c(28) = 0.218d^{0.444} \quad R^2 = 0.991 \tag{vi}$$

Due to the absence of a predictive model for computing the compressive strength of geopolymers, especially those incorporating SFA as the coarse aggregate, utilizing the compressive strength at 28 days with curing age, the proposed predictive model values are validated using a well-established concrete curing age estimation model [9].

Table 7. Existing estimating compressive strength models based on curing time

S. No.	Strength Prediction Model	
(a)	$F_c(d) = \frac{d * F_c(28)}{4 + 0.85d}$	; ACI-209, 1992 [11]
(b)	$F_c(d) = 1 \cdot 11 \frac{d * F_c(28)}{4 \cdot 5 + 0.85d}$	; JSCE, 2007 [11]
(c)	$F_c(d) = \exp\left(0.25 \left(1 - \sqrt{\frac{28}{d}}\right)\right) * F_c(28)$	; Eurocode-2, 2007 [13]
(d)	$F_c(d) * F_c(28)$	; JCI, 2008 [15]

lists worldwide strength prediction models for determining compressive strength based on 28-day compressive strength and curing time show in Table 7.

### Conclusion

The present study rigorously explored the viability of replacing traditional aggregate with Sintered Fly ash (SFA) in geopolymer concrete, with a specific focus on the impact of diverse particle sizes. By constructing a regression-based model using experimental compressive strength data at different curing times, the study facilitated an evaluation of compressive strength about specific packing densities. Comparative analyses were conducted with several other concrete strength prediction models. The key conclusions drawn from this investigation include:

- The utilization of 100% SFA as coarse aggregate in geopolymer concrete, illustrated by sample A2 with aggregate yielded favorable results, achieving the targeted compressive strength within 28 days.
- A2, featuring a packing density of exhibited improved packing density results compared to A1, A3, A4, and A5.
- The proposed model demonstrated reliability in predicting compressive strength in geopolymer concrete, irrespective of packing density.
- Thin section analysis revealed a more robust aggregate-matrix interface due to the porous structure of sintered fly ash aggregate.

- It is recommended to use SFA as coarse aggregate in geopolymers to enhance environmental stability, promote sustainability in construction with lightweight cement-free concrete, and reduce waste (such as fly ash) while minimizing the impact of mining natural aggregates. Geopolymer concrete, compared to Portland cement, proves to be a more environmentally friendly alternative.

#### CONFLICTS OF INTEREST

The authors declare that they have no competing interests.

#### REFERENCES

- [1] Aldawsari S, Kampmann R, Harnisch J, Rohde C. Setting time, microstructure, and durability properties of low calcium fly ash/slag geopolymer: a review. *Materials*. 2022 Jan 24;15(3):876. <https://doi.org/10.3390/ma15030876>
- [2] Amin M, Elsakhawy Y, Abu el-hassan K, Abdelsalam BA. Behavior evaluation of sustainable high strength geopolymer concrete based on fly ash, metakaolin, and slag. *Case Studies in Construction Materials*. 2022 Jun 1;16:e00976. <https://doi.org/10.1016/j.cscm.2022.e00976>
- [3] Chu HH, Khan MA, Javed M, Zafar A, Khan MI, Alabduljabbar H, Qayyum S. Sustainable use of fly-ash: Use of gene-expression programming (GEP) and multi-expression programming (MEP) for forecasting the compressive strength geopolymer concrete. *Ain Shams Engineering Journal*. 2021 Dec 1;12(4):3603-3617.
- [4] Domagała L. Durability of structural lightweight concrete with sintered fly ash aggregate. *Materials*. 2020 Oct 14;13(20):4565.
- [5] Gupta G, Sood H, Gupta PK. Mathematical modelling of resilient modulus response of fibre reinforced clay subgrade for pavement design. *Journal of Interdisciplinary Mathematics*. 2020 Jan 2;23(1):247-255.
- [6] Hamidi F, Valizadeh A, Aslani F. The effect of scoria, perlite and crumb rubber aggregates on the fresh and mechanical properties of geopolymer concrete. In *Structures 2022* Apr 1;38:pp. 895-909. Elsevier.
- [7] Jena S, Panigrahi R. Performance assessment of geopolymer concrete with partial replacement of ferrochrome slag as coarse aggregate. *Construction and Building Materials*. 2019 Sep 30;220:525-537.
- [8] Kuranlı ÖF, Uysal M, Abbas MT, Cosgun T, Niş A, Aygörmez Y, Canpolat O, Al-Mashhadani MM. Evaluation of slag/fly ash based geopolymer concrete with steel, polypropylene and polyamide fibers. *Construction and Building Materials*. 2022 Mar 28;325:126747. <https://doi.org/10.1016/j.conbuildmat.2022.126747>
- [9] Miao R. High technology investment risk prediction using partial linear regression model under inequality constraints. *Journal of Interdisciplinary Mathematics*. 2018 May 19;21(4):869-881.
- [10] Pham TM, Lim YY, Malekzadeh M. Effect of pre-treatment methods of crumb rubber on strength, permeability and acid attack resistance of rubberised geopolymer concrete. *Journal of Building Engineering*. 2021 Sep 1;41:102448. <https://doi.org/10.1016/j.job.2021.102448>
- [11] Pham TM, Liu J, Tran P, Pang VL, Shi F, Chen W, Hao H, Tran TM. Dynamic compressive properties of lightweight rubberized geopolymer concrete. *Construction and Building Materials*. 2020 Dec 30;265:120753. <https://doi.org/10.1016/j.conbuildmat.2020.120753>
- [12] Shi J, Liu Y, Wang E, Wang L, Li C, Xu H, Zheng X, Yuan Q. Physico-mechanical, thermal properties and durability of foamed geopolymer concrete containing cenospheres. *Construction and Building Materials*. 2022 Mar 28;325:126841. <https://doi.org/10.1016/j.conbuildmat.2022.126841>
- [13] Soni N, Shukla DK. Analytical study on mechanical properties of concrete containing crushed recycled coarse aggregate as an alternative of natural sand. *Construction and building materials*. 2021 Jan 10;266:120595. <https://doi.org/10.1016/j.conbuildmat.2020.120595>
- [14] Tayeh BA, Hakamy A, Amin M, Zeyad AM, Agwa IS. Effect of air agent on mechanical properties and microstructure of lightweight geopolymer concrete under high temperature. *Case Studies in Construction Materials*. 2022 Jun 1;16:e00951. <https://doi.org/10.1016/j.cscm.2022.e00951>
- [15] Tayeh BA, Zeyad AM, Agwa IS, Amin M. Effect of elevated temperatures on mechanical properties of lightweight geopolymer concrete. *Case Studies in Construction Materials*. 2021 Dec 1;15:e00673. <https://doi.org/10.1016/j.cscm.2021.e00673>
- [16] Top S, Vapur H, Altiner M, Kaya D, Ekicibil A. Properties of fly ash-based lightweight geopolymer concrete prepared using pumice and expanded perlite as aggregates. *Journal of Molecular Structure*. 2020 Feb 15;1202:127236. <https://doi.org/10.1016/j.molstruc.2019.127236>
- [17] Zeyad AM, Magbool HM, Tayeh BA, de Azevedo AR, Abutaleb A, Hussain Q. Production of geopolymer concrete by utilizing volcanic pumice dust. *Case Studies in Construction Materials*. 2022 Jun 1;16:e00802. <https://doi.org/10.1016/j.cscm.2021.e00802>